Jitter Models and Measurement Methods for High-Speed Serial Interconnects

Andy Kuo[1], Touraj Farahmand[1], Nelson Ou[1], Sassan Tabatabaei[2], André Ivanov[1]
[1]*SoC Research Group, University of British Columbia*
[2]*Guide Technology, Sunnyvale, CA*
andyk@ece.ubc.ca, tourajf@ece.ubc.ca, nelsonou@ece.ubc.ca, sassan@guidetech.com, ivanov@ece.ubc.ca

Abstract*—*Jitter can be decomposed into several subcomponents, each having specific sets of characteristics and root-causes. This paper focuses on describing causes and measurement methods of jitter subcomponents. We first describe the relationship between a jitter PDF and bit error rate (BER) followed by a discussion on what causes jitter. Common jitter measurement methods are presented, along with an analysis of their respective advantages and disadvantages. Our recent research on the cause and practical measurement results and design issues of bounded uncorrelated jitter (BUJ), a subcomponent of jitter, due to crosstalk, is also presented.

I. INTRODUCTION

The recent deployment of Gb/s serial I/O interconnects aims at overcoming data transfer bottlenecks arising with parallel bus architectures, e.g., limited ability to increase chip pin counts. Gb/s data rates of today's asynchronous IO introduce new signal integrity issues as shown in Figure 1. Such signal integrity issues include ringing, reflection, EMI, ground bounce, switching power supply noise, thermal noise, and crosstalk.

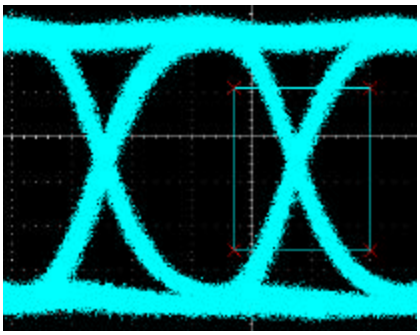

Figure 1: Signal Integrity Illustration [1]

Traditionally, the performance of a communication link has been measured by its associated *bit error rate* (BER), which is the ratio of the number of bits received in error to the total number of bits transmitted. When data rates increase, the jitter magnitude and signal amplitude noise need to decrease proportionally in order to maintain an acceptable BER. At data rates in excess of 1Gb/s, a slight increase in jitter or amplitude noise will have a much more pronounced effect on the BER than at lower data rates. Specifying jitter and noise simply through peak-to-peak or RMS values is deemed to be inadequate [1]. Jitter peak-to-peak value is sample size-dependent and requires impractically long time to measure in the presence of random noise. This is because, by definition, random noise is unbounded due to its Gaussian distribution nature. A fast peak-to-peak jitter measurement is ambiguous unless some boundary condition is established. While some jitter components can be characterized fully through an RMS value, the same does not hold for deterministic jitter due to its varying *probability density function* (PDF). Therefore, describing jitter simply via an RMS value is insufficient for accurately estimating a link's BER performance. Moreover, a simple RMS or peak-to-peak value cannot sufficiently describe the characteristics of different types of jitter and their impact on a link's performance. Overall, more accurate jitter and noise models are required, to allow better predictions and characterizations of devices subject to jitter effects. Clearly, there is a need for accurate jitter and noise analysis methods to allow accurate and required predictions and characterizations of devices subject to jitter effects.

One difficulty with jitter analysis is identifying the different jitter components contributing to the total jitter. Currently, various jitter analysis methods exist, such as the TailFit algorithm, and spectral methods, to name just a few. The TailFit algorithm is a de-convolution method capable of separating total jitter into its random and deterministic components [2][3][4]. Another method uses a real-time sampling oscilloscope to capture the signal information and compute the time deviation in each edge transition of a data stream. Jitter parameters can then be extracted. Deterministic jitter can be further decomposed to model the different impacts of its subcomponents on the link performance to identify the root cause and thereby enable design strategies aimed at reducing jitter.

The remainder of this paper is organized as follows. Section II provides strict definitions for total jitter and jitter sub-components. In addition, the relationship between jitter probability density function (PDF) and BER is also discussed. Sections III looks at causes of random (RJ) and deterministic (DJ) jitter. Section IV presents various jitter measurement methods. Section V presents the highlight of our recent BUJ research. Finally, our conclusions are drawn in Section VI.

[1] Measurement taken from System on a Chip (SoC) Test Lab, University of British Columbia.

II. JITTER DEFINITION

Jitter is defined as the deviation of a timing event of a signal from its intended (ideal) occurrence in time, as shown in Figure 2(a). A timing event is usually the rising and/or falling edge of the signal. Traditionally, an *eye diagram is* used to specify signal integrity limits including jitter, as shown in Figure 2(b). Jitter can be expressed in absolute time or normalized to a unit interval (UI). A UI is the ideal or average time duration of a single bit or the reciprocal of the average data rate. An eye diagram is a composite of all the bit periods of the captured bits superimposed on each other relative to a bit clock (recovered or available from the source). The open area within the eye is referred to as the eye opening. So-called *eye masks* can be constructed from specific protocol AC and DC specifications. Such eye masks can represent the minimum signal requirements at the transmitter output or at the receiver input. In device characterization stages, an eye mask can be fitted over an eye opening to show signal compliance to a protocol. Any signal crossing the eye mask is considered to violate the specification.

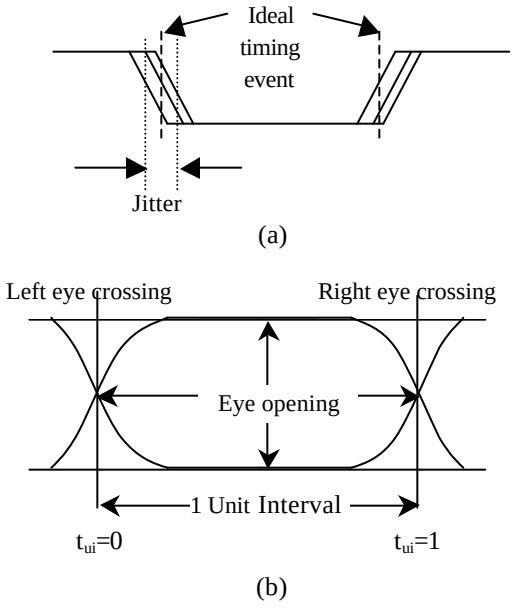

Figure 2: Jitter (a) and Eye Diagram (b).

2.1 Jitter Subcomponents

Jitter can be subdivided into two categories: random jitter and deterministic jitter (DJ) [3][6][7][8]. Figure 3 shows taxonomy of the total jitter subcomponents [3].

The jitter specifications of a serial communication link normally specify total jitter (TJ) and either or both RJ and DJ.

RJ is a random process, which is generally divided into Gaussian and non-Gaussian distributions. Most experts/practioners tend to assume RJ to be a Gaussian distribution because most noise sources have Gaussian distributions.

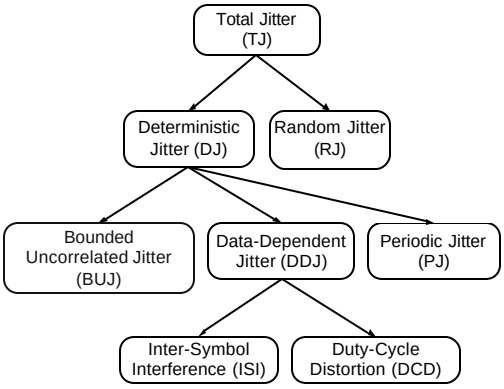

Figure 3: Jitter subcomponents.

Deterministic jitter is in turn comprised of the following subcomponents.

Data-Dependant Jitter (DDJ)

DDJ corresponds to a variable jitter that is dependent on the bit pattern transmitted on the link under test. DDJ can in turn classify into two sub-components: *Duty-Cycle Distortion (DCD)* and *Inter-Symbol Interference (ISI)*. DCD describes a jitter amounting to a signal having unequal pulse widths for high and low logic values. ISI is jitter that is dependent on the transmitted patterns on the same trace.

Sinusoidal Jitter/Periodic Jitter (PJ)

PJ refers to periodic variations of signal edge positions over time.

Bounded Uncorrelated Jitter (BUJ)

BUJ is typically due to coupling, e.g., from adjacent data-carrying links, or on-chip random logic switching [8]. BUJ is bounded due to finite range coupling effect on signal transitions, and uncorrelated because there is no correlation between the signal transitions of the adjacent links. The exact model depends on the data pattern, coupling signal, and coupling mechanism.

2.2 Jitter Probability Density Function and BER

The PDF of TJ is the convolution of its RJ and DJ components [9]. Conversely, RJ and DJ can be separated from TJ through de-convolution [9]. Similarly, the PDFs of the jitter subcomponents can also be convolved to form the PDF of total DJ. Both convolution and de-convolution processes require RJ and DJ components to be described by their PDFs rather than through simple peak-to-peak values because jitter can generally be viewed as a stochastic process. In most practical cases RJ can be characterized by a Gaussian distribution function [3][7][8][9]. DJ is assumed bounded and can have a variety of PDFs determined from the aggregate of its subcomponents.

The TJ PDF can be used to estimate the bit error rate (BER) [1]. That is, the BER is essentially the cumulative distribution function (CDF) of the TJ PDFs of the left and right eye crossings over the time interval where a bit error occurs.

III. CAUSES OF JITTER

In this section, we discuss in more detail the causes of different jitter sources. We discuss the causes for each jitter subcomponents. The section is divided into two subsections; the first subsection discusses the causes of RJ, the second subsection discusses the causes of DJ.

3.1Causes of Random Jitter (RJ)

The causes of RJ are generally due to device noise sources, e.g., thermal noise and flicker noise [3][4]. An example of device noise is shot noise, which is related to the fluctuation in current flow in a transistor. Another component of device noise is thermal noise. Electron scattering causes thermal noise when electrons move through a conducting medium and collide with silicon atoms or impurities in the lattice. Higher temperatures results in greater atoms vibrations and increases chances of collisions. Flicker noise, or 1/frequency noise, is caused by the random capture and emission of carriers from oxide interface traps affecting carrier density in a transistor [3].

3.2 Causes of Deterministic Jitter (DJ)

DJ arises from the interaction of different specific system components. Major causes for DJ include electromagnetic interference (EMI), crosstalk, signal reflection, driver slew rate, skin effect and dielectric loss [4,6]. EMI is the interference from energy radiated or conducted from other devices or systems. EMI radiation can induce currents on signal wires and power rails, and alter the signal voltage biases or the reference voltages.

Impedance mismatch between the cables/traces and a terminating resistor contribute to the occurrence of signal reflections. As a signal propagates and reaches the receiver end, part of the signal energy is reflected back towards the transmitter. The fraction of the reflected energy relative to the signal energy can be estimated by the following [11]

$$\%_{reflect} = \frac{Z_L(w) - Z_o(w)}{Z_L(w) + Z_o(w)} * 100\%$$

where Z_L is the load impedance, Z_o is the wire impedance, and ? is the angular frequency of the transmitter signal. Electrons literally bounce back to the transmitter when mismatches in the terminating resistance occur. The result is the corruption of the succeeding bits and reduction in the signal-to-noise ratio (SNR). The reflected signal energy bounces back and forth until it is completely dissipated. As the reflected signal bounces back and forth, it adds to the original signal, resulting in jitter. Note that if a source side termination resistor is used and has matching resistance, then the reflected signal will be absorbed and no data corruption will occur. Because the impact of reflected signal depends on the data pattern being transmitted, signal reflection can be considered as part of the DDJ.

Above a certain frequency, skin effect occurs in the transmitting conductors. The skin effect is a phenomenon where the current flow tends to concentrate on the surface of a conducting medium at high frequencies due to conductor self-inductance. The on-set frequency is a function of the conductor's cross-sectional area, impedance, and other material physical parameters [10][11]. The skin effect increases the conductor resistance due to reduced effective cross-section area, which leads to increased attenuation of the high frequency contents of a signal. The results are longer rise and fall times and degraded signal amplitudes.

Dielectric loss is due to the delay of polarization in the dielectric material when it is subject to a changing electric field. In an ideal lossless material, the current leads the voltage by 90 degrees, but in a real material, the delay in polarization results in a phase lag between the external electric field and the resonating molecules. This leads to a phase difference in current and amounts to power loss. Above some frequencies, dielectric losses dominate the skin effect losses because dielectric losses are proportional to the frequency while skin effect losses are proportional to the square root of the frequency [10].

The frequency dependency of the skin effect and dielectric losses make them causes of DDJ. The attenuations due to the skin effect and dielectric losses contribute to the vertical closure of the signal eye diagram. The attenuations also contribute to slower rise/fall rates, which reduce the horizontal eye opening.

The signal slew rate depends on the signal driver's ability to drive its load. A strong driver can provide a fast slew rate and is able to drive higher frequency signals. When a weak driver is used to drive a high frequency signal, the signal at the opposite end of the wire may not have enough time to rise or fall to the desired signal high or low value. Using a linear phase FIR filter with cut-off frequency at 1GHz to emulate a driver, Figure 4 illustrates the slew rate limitation when transmitting a data pattern at 3GHz.

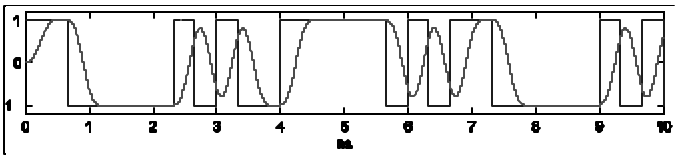

Figure 4: Driver slew rate limitation

Crosstalk is the main cause of BUJ. Crosstalk refers to the interference from other signal traces. The injected crosstalk noise onto the victim travels both backward towards the near end and forward towards the far end on the victim as shown in Figure 5. As the data bit travels through the aggressor, the rising and falling edge of the bit continuously introduce noise onto their neighboring victim.

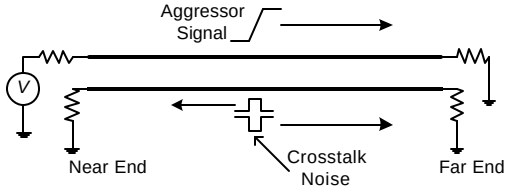

Figure 5: Crosstalk noise induced from aggressor

There is also a secondary crosstalk effect. Once a crosstalk signal has been induced to the victim, this pulse wave on the victim conductor can act as an aggressor and inject a noise signal back to the original conductor. This is called *strong* coupling if this secondary effect is strong and *weak* coupling if the effect can be ignored.

Table 1 summarizes the effect of crosstalk noise on different switching edges at the far and near ends of the victim conductor.

Edge Transition	Mutual Capacitance		Mutual Inductance	
	Near End	Far End	Near End	Far End
Rising Edge	Positive Pulse	Positive Pulse	Positive Pulse	Negative Pulse
Falling Edge	Negative Pulse	Negative Pulse	Negative Pulse	Positive Pulse

Table 1: Effect of mutual capacitance and mutual inductance on the polarity of crosstalk noise

In reality, mutual capacitance and inductance are always present. Assuming a weakly coupled system, there will be some cancellation between capacitive and inductive crosstalk on the far end due to opposite polarities of the pulse generated. The amount of cancellation depends on the amount of mutual inductance and capacitance. On the other hand, cancellation is not possible at the near end and will be more severe.

The amount of crosstalk depends on the signal amplitude, the trace/cable length, the trace/cable separation and the edge transition time of the aggressor. Large aggressor signal amplitude, long trace length, narrow trace separation, and fast aggressor rise/fall time can contribute to higher crosstalk. Crosstalk alters the voltages of the affected signal wires, which affect the edge transition times of the signals and result in jitter. A custom PCB is designed and manufactured for BUJ experiment that includes 16cm long parallel traces in microstrip configuration. With our custom PCB setup, the inductive effects are greater than the capacitive ones. Hence, at the far end, if both the aggressor and victim switch in the same direction, the switching is slower than ideal. If the aggressor and victim switch at different direction, the coupling will have the apparent effect of increasing the speed capability of the design.

The distance between traces also has an important effect. Figure 6 shows histograms of jitter measured from real-time oscilloscope due to BUJ. In this figure, RJ is unavoidably included due to practical measurement. Figure 6(b) has spacing between two traces twice as much as the spacing in Figure 6(a). In Figure (6)a, the jitter from the rightmost peak to the leftmost peak, also defined here as *peak-to-peak jitter*, corresponds to a time interval of 34.7ps whereas in Figure (6)b, the peak-to-peak time interval is only 20.4ps. This agrees with the trend that as the spacing between traces moves further apart, the amount of coupling reduces.

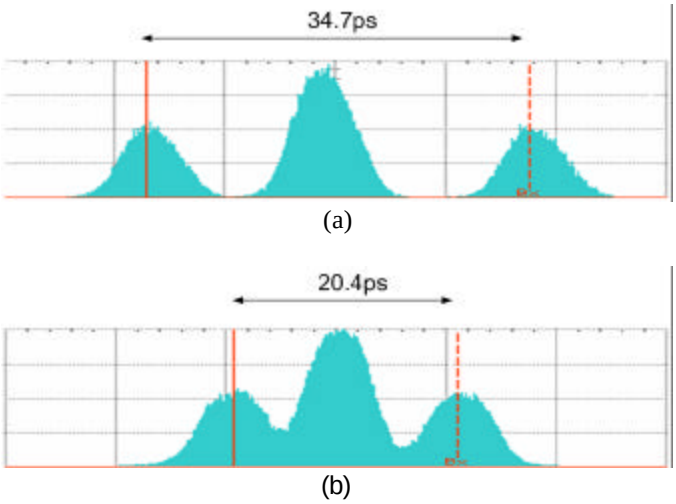

Figure 6: Histogram of BUJ and RJ with one aggressor (K28.5 data pattern) and victim setup: a) 1x spacing, b) 2x spacing[2].

IV. JITTER MEASUREMENT METHODS FOR JITTER SUBCOMPONENTS

While some applications tolerate that certain jitter components be ignored, most common applications require that the majority of jitter components be considered and therefore be carefully measured and characterized. Many jitter measurement methodologies using different equipment, including Time Interval Analyzers (TIAs), oscilloscopes, and BER Testers (BERTS), are used in practice or have been proposed in literature. Describing all such methods in detail is beyond the scope of this paper. In Table 2, we list some of the key jitter model characteristics that have been used to measure jitter components to illustrate the application of jitter models in test and measurement. Jitter measurement methods are presented to show how different jitter measurement methods use jitter models in general. Readers are encouraged to read the relevant references for more information.

4.1 Random Jitter (RJ) Measurement

RJ can be measured using several methods. Assuming the signal to be a simple clock-like pattern and that there are no DJ components, RJ can be estimated from captured histograms. In the presence of other jitter components or when a non-clock like data pattern is being transmitted, other methods for measuring RJ are required. One such method is to use curve-fitting algorithms. Because the tails of a jitter histogram are populated by Gaussian random jitter components even when in the presence of DJ, curve fitting algorithms try finding best Gaussian fits to the tail regions. An RJ estimate is provided by the standard deviation of the matched Gaussian distribution [2]. However, there are limitations to this method. Firstly, a large number of samples are required to be able to fit Gaussian PDF on

[2] Measurement taken from System on a Chip (SoC) Test Lab, University of British Columbia with Agilent Infiniium 54856 Series 20GHz Bandwidth Real Time Oscillscope

the tails accurately. Secondly, non-Gaussian jitter cannot be decomposed.

Jitter type	Model Properties	Measurement methods	Equipment
RJ	Gaussian distribution	TIE (Time Interval Error) measurement and PDF or histogram tail fit	Real time sampling oscilloscope, TIA
		BER bathtub curve	BERT
	Random nature (any distribution)	Frequency domain	Spectrum analyzer
		TIE measurement and frequency domain analysis	Real time sampling oscilloscope, TIA
		Under-sampled TIE measurement and frequency domain analysis	TIA, oscilloscope
DDJ	Discrete delta lines in PDF	TIE, histogram	Real time sampling oscilloscope, BERT
	Deterministic TIE variation from edge to edge	TIE measurement with edge lock method and averaging in time domain	Real time sampling oscilloscope, TIA
	Repetitive nature when the pattern is repeated	TIE measurement and frequency domain analysis	Real time sampling oscilloscope
PJ	PDF or histogram shape	TIE or time interval histogram	Real time sampling oscilloscope
	Periodic nature	TIE measurement and autocorrelation estimation method, Hilbert transform method	TIA, oscilloscope
BUJ	Bounded PDF	Use general PDF-based DDJ measurement method	Real time or equvalent-time sampling oscilloscope, TIA

Table 2: Measurement Methods and Equipments

Another method for measuring RJ requires a spectral analysis by performing a Fourier transform on captured data to reveal the spectral content of the jitter signal. Because RJ is stochastic, it exhibits on the spectral graph as small amplitude noise floor across all frequencies. The RMS value of the noise floor is the RJ RMS value [13]. Figure 7 shows an example of spectral analysis with RJ and PJ (top) and RJ only (bottom).

With BERT measurements, RJ can be calculated using the slope of the BER bathtub curves, which represent the jitter CDF. However, such jitter estimates tend to overestimate RJ [6]. This method can only separate RJ assuming RJ is a Gaussian distribution.

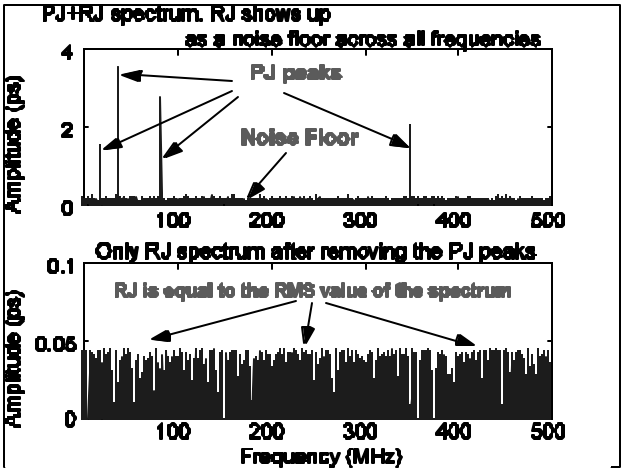

Figure 7: Spectral analysis of PJ + RJ (top) and RJ only (bottom)

4.2 Deterministic Jitter (DJ) Measurement

By transmitting a clock-like data pattern, DCD can be measured directly by measuring the periods of logic high and logic low. ISI does not exist in this case while RJ can be averaged out with large number of samples. Using the same clock-like data pattern, the peak-to-peak PJ can also be estimated on the histogram. The histogram captured by an oscilloscope or a TIA contains both RJ and PJ components. Since the tail portions are the RJ components, PJ can be estimated by simply measuring the peak-to-peak separation in the histogram [6]. This method works for single-tone sinusoidal PJ. With multiple-tone sinusoidal PJ, measuring peak-to-peak separation in the histogram will not be adequate.

ISI jitter can be measured by transmitting a data pattern containing both long and short bit run lengths. The ideal timing event for the i_{th} edge in the pattern relative to a reference edge would occur at n*UI, while an actual timing event may contain deviations which can be expressed as n*UI + X_i, where X_i denotes the displacement of the i_{th} edge. Using devices such as a TIA that can accurately measure the time between two timing events, one can measure X_i for each edge. The measured X_i values contain random and periodic components, which can be removed by averaging. The distribution of averaged X_i is the ISI PDF. The limitation of this method is that it needs a repeating pattern and low frequency PJ might not average out, therefore show up in the measurement results, and reduce the accuracy.

Another way of measuring PJ, DCD, and ISI, is through spectral analysis. Since a PJ component has fixed frequency components, it will appear in the spectral graph as a large magnitude peak. PJ jitter magnitude can be computed by an inverse Fourier transform after it is isolated from all other jitter components in the spectral graph. Because DCD and ISI are

pattern dependant, they must show up in the spectral graph at multiples of fr/N (fr=bit rate), where N is the data pattern length [13]. The method described in [13] amounts to first performing an inverse transform of the combined components, then constructing a histogram for each of the rising and falling edges. The difference between the mean values of the two histograms is the DCD, while the difference between the peak-to-peak values of the histogram corresponds to ISI. From the above measurement methods, jitter PDFs can be specified. TJ of the serial communication system under measurement is then a convolution of all the jitter PDFs. Spectral analysis can easily separate RJ from TJ if assuming RJ has a Gaussian distribution. It is also very simple to identify PJ components. However, it is very difficult to separate BUJ and subcomponents of DDJ.

Instruments used in jitter measurement have certain characteristics that make certain ones better for certain types of applications. A fast real-time sampling oscilloscope acquires as many samples as possible on a signal in one pass and reconstructs the signal waveform for display by interpolation. In such cases, the acquired data is compared to the clock recovered from the signal bit stream by a golden CDR circuit to determine the timing error of each edge. The resulting set of error values is then used for spectrum analysis [2]. A Real-time oscilloscope can also construct a waveform eye diagram and fit waveform eye masks. One advantage of this method is that specific edge transition behavior can be analyzed individually and constructed to provide a good analysis of DJ. However, a real-time sampling oscilloscope generally does not have a very high frequency bandwidth.

Another type of oscilloscope, the *equivalent time sampling oscilloscope* (ET-DSO), acquires only one sample for each trigger event and reconstructs the signal waveform by overlaying different samples captured over the multiple trigger events [2]. The equivalent time oscilloscope provides very low intrinsic jitter, which is helpful for measuring RJ accurately if trigger signal has low jitter, and highest front-end bandwidth available in today's instruments, which minimizes the instrument impact on DDJ measurement accuracy. An ET-DSO, however, requires a repeating signal pattern and a triggering signal to control the sampling process. An ET-DSO can measure signals running at frequencies higher than its sample rate, but its disadvantage is its low acquisition speed and difficulty in acquiring non-coherent noises. An ET-DSO can construct waveform eye diagrams as well. Unlike real-time oscilloscopes, equivalent time oscilloscopes suffer from trigger jitter because multiple triggers are used [2]. Another drawback of equivalent time sampling oscilloscopes is that specific edge transitions behavior cannot be analyzed individually. Therefore, it is difficult to separate RJ from TJ if DJ exists that may be present in the signal under test.

A TIA can operate with or without a clock (generated from a golden PLL) or a pattern marker. A TIA uses many single-shot edge-to-edge time measurements rather than extrapolating acquired signal samples to get the timing information. Spectrum analysis can be performed on the data set acquired by a TIA. Using a TIA is fast because it collects only edge timing information that carries jitter information. With a pattern marker or event counter, jitter subcomponents can be reliably separated. However, in a real system environment, pattern marker is difficult to generate.

A BERT measures the bit-error-rate of a signal at a certain point in the transmission link. A BERT needs to be clocked by a golden CDR circuit driven by the signal under test. A BERT varies the sampling instant with respect to the clock edges over the entire bit time and measures the BER. The resulting plot of BER vs. time is referred to as the bathtub plot, which provides a direct measurement of TJ. Longer measurement time yields lower BER and hence better accuracy. However, the apparent constraint on test time limits the BERs performance in practice. Currently, there exist curve extrapolation techniques that use statistical jitter models to extend the measured BER to lower values without incurring unfeasible test times. There exist methods that use jitter models to separate RJ and DJ components from the bathtub curve [6]. However, this method of testing requires a long test time to measure a low BER. It may take hours to measure for a 10^{-12} BER. This method of extrapolating TJ into RJ and DJ is relatively accurate and generally correlates well to the results from a TIA-based method with pattern marking. However, DJ results maybe slightly smaller due to approximations.

V. Bounded Uncorrelated Jitter Measurement Highlights

From Figure 6, we can see that when measuring crosstalk to find out the histogram of BUJ, there are also other jitter components to deal with. One way to isolate other jitter component to find out the BUJ is to look at each edge specifically. In [14], our previous published work, RJ and PJ each has a symmetrical PDF shape. Assuming there is no DDJ, we can look at each victim's edge correspond to the aggressor's specific switching edge and average out the difference to establish three solid delta function-like lines as shown in Figure 8. In Figure 8, the histogram data is taken at the victim's falling edge of the clock at 2Gb/s. The aggressor has a data rate of 1Gb/s with K28.5 data pattern. The leftmost delta line refers to the fact that the aggressor and victim switch in different directions, i.e. aggressor switches from logic 0 to 1 and victim switch from logic 1 to 0. On the other hand, the rightmost delta line illustrates the case where both aggressor and victim lines switch in the same direction, i.e. both aggressor and victim switching from logic 1 to 0. The middle delta line occurs from the cases where there is no switching in the aggressor and hence no coupling effect on the victim edge, i.e. aggressor pattern has a bit sequence of 00 or 11. The relative occurrence of such aggressor edge transitions is larger than that of the others and hence results in a higher number of occurrences.

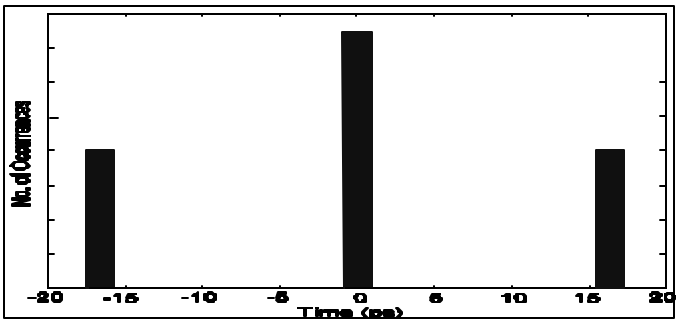

(a)

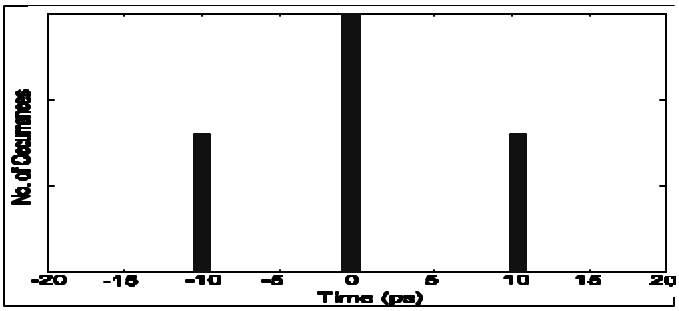

(b)

Figure 8: Histogram of BUJ (RJ isolated) with one aggressor (K28.5 data pattern) and one victim setup: a) 1x spacing, b) 2x spacing.

Figure 8 showed the histogram of BUJ for a configuration comprised on only two parallel traces. Figure 9 shows the histogram of a three parallel trace configuration with the middle trace as the victim and the two aggressors at the sides carrying identical signals. Because both aggressors switch at the same time, the effects of time deviations on the victim signal are amplified in comparison to the single trace configuration.

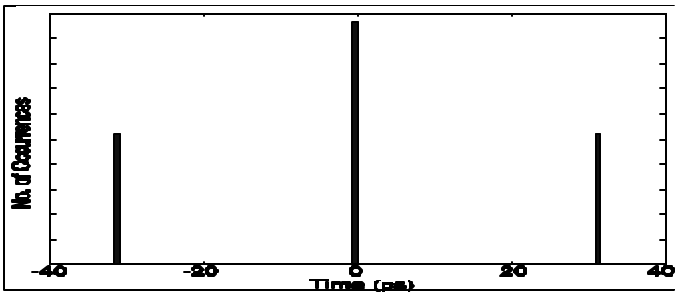

Figure 9: Histogram of BUJ (RJ isolated) with two aggressors (both K28.5 data patterns) and one victim sandwiched between two aggressors carrying identical data patterns.

We investigated the case where the configuration consisted of five parallel traces and where the aggressors carried different signal patterns. Figure 10 shows a histogram for such a configuration. There are more delta lines due to the different switching conditions, i.e., aggressor 1 switching from logic 0 to 1, aggressor 2 not switching, and aggressor 3 switches from logic 1 to 0, aggressor 4 not switching. From the figure, the delta lines have higher amplitude towards the center of the plot compared to delta lines away from the center. The delta line farthest away to the left and right are due to rare occurrences. For example, a logic 0 to 1 transition for all four aggressors is rarely to occur. The middle delta line has much larger amplitude due to more occurrences. This does not mean only all of the aggressors are not switching, it also means that the effect from the aggressors cancels each other out. For example, the two aggressors located on the left side of the victim have logic 0 to 1 transitions while the two aggressors located on the right side of the victim have logic 1 to 0 transitions. From these histograms, we have illustrated how it is possible to predict the PDF of the patterns from the knowledge of the different switching characteristics of each aggressor and combining the effect.

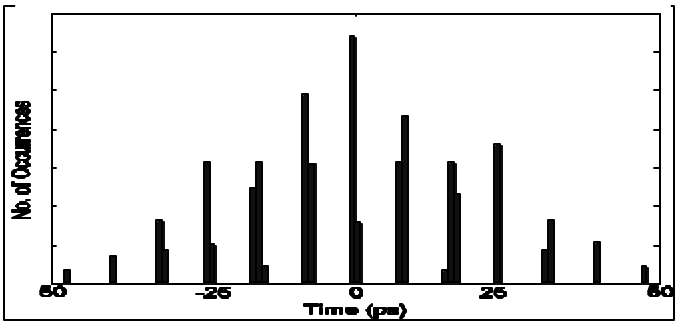

Figure 10: Histogram of BUJ (RJ isolated) with four aggressors carrying different data patterns (PRBS7, PRBS5, K28.5 and clock signal) and one sandwiched victim.

VI. CONCLUSION

This paper focuses on the important problem of jitter. We presented a useful taxonomy of jitter components and discussed their general characteristics and root causes. We showed the necessity for describing jitter components using probability distribution functions. We also presented various jitter measurement methods that exploit the jitter models presented toward jitter analysis and decomposition. Measurement methods accuracy, advantages and disadvantages were also highlighted. Finally, some investigation results into the characterization of BUJ were presented briefly. Detail methodology and mathematic models is still in progress and will be available in the future.

ACKNOWLEDGMENT

The authors would like to acknowledge contributions from the following UBC SoC Research Lab members for their valuable discussions and suggestions: Dr. Roberto Rosales, James Cicalo and A.K.M. Kamruzzaman Mollah. The authors would also like to thank local Vancouver office of Agilent Technologies Inc. for their support on providing us access to various test equipments.

REFERENCES

[1] Mike Li, Jan Wilstrup, "Paradigm Shift for Jitter and Noise in Design and Test > 1Gb/s Communication Systems" IEEE International Conference on Computer Design, 2003.

[2] Secretariat International Committee for Information Technology Standardization (INCITS), T11.2/Project 1316 DT/Rev 10.0, "Fiber Channel - Methodology for Jitter and Signal Quality Specification-MJSQ," March 10, 2003.

[3] John Patrin, Mike Li, "Comparison and Correlation of Signal Integrity Measurement Techniques," DesignCon 2002.

[4] *Jitter Analysis Techniques for High Data Rates*, Agilent Technologies Inc., Application Note 1432, February 2003 [Online], Available: http://cp.literature.agilent.com/litweb/pdf/5988-8425EN.pdf.

[5] Yi Cai, Bernd Laquai, Kent Luehman, "Jitter Testing for Gigabit Serial Communication Transceivers," *IEEE Design and Test of Computers*, Vol.9, Issue1, January 2002, pp. 66-74.

[6] Yi Cai, S.A. Werner, G.J. Zhang, M.J. Olsen, R.D. Brink, "Jitter Testing for Multi-Gigabit Backplane SerDes," *Proc. International Test Conference* (ITC 02), IEEE Press, Piscataway, N.J., Sept. 2002, pp700-710.

[7] *Understanding Jitter*, WAVECREST Corporation, 2001 [Online], Available: http://www.wavecrest.com/technical/VISI_6_Getting_Started_Guides/6understanding.PDF.

[8] *Jitter in Digital Communication Systems, Part 1*, MAXIM Integrated Products, Application Note HFAN-04.0.3, Rev0, September 2001 [Online], Available: http://pdfserv.maxim-ic.com/en/an/5hfan403.pdf.

[9] J. Sun, M. Lee, J. Wilstrup, "A Demonstration of Deterministic Jitter (DJ) Deconvolution," in *Proc. 19th IEEE Instrumentation and Measurement Technology Conference (IMTC 2002)*, Anchorage, AK, 2002, pp. 293-298.

[10] H. W. Johnson, M. Graham, *High-Speed Signal Propagation: Advanced Black Magic*, New Jersey: Prentice Hall, 2003.

[11] H. W. Johnson, M. Graham, *High-Speed Digital Design: A Handbook of Black Magic*, New Jersey: Prentice Hall, 1993.

[12] B. Young, *Digital Signal Integrity, Modeling and Simulation with Interconnects and Packages*, Upper Saddle River, NJ: Prentice Hall, 2001, pp. 98-104, 200-207.

[13] *Understanding and Characterizing Timing Jitter*, Tektronix Inc., Application Note, 2003 [Online], Available: http://www.tektronix.com/jitter

[14] N. Ou, T. Farahmand, A. Kuo, S. Tabatabaei, and A. Ivanov, "Jitter Models for the Design and Test of High-Speed (Gb/s) Serial Interconnects," *IEEE Design and Test of Computers*, vol. 21, Jul-Aug 2004.